(2)

AEW TR 76003
Copy No 35

BR52460

AEW

THE DRAG OF AN ACCELERATING SUBMARINE PART I SKIN FRICTION (U)

T B Booth

ADMIRALTY EXPERIMENT WORKS
HASLAR GOSPORT
HAMPSHIRE PO 12 2AG

PROCUREMENT EXECUTIVE
MINISTRY OF DEFENCE

AEW TR 76003

January 1976

ADMIRALTY EXPERIMENT WORKS, HASLAR

(12) 2 p.

(4) AEW TECHNICAL REPORT, 76003

(14) AEW-TR-76003

(6) THE DRAG OF AN ACCELERATING SUBMARINE. PART I. SKIN FRICTION. (U)

DRI-1

(19) BR-52416

(10) BY T. B. BOOTH

(11) JAN[redacted]1976

PROCUREMENT EXECUTIVE
MINISTRY OF DEFENCE

60/12

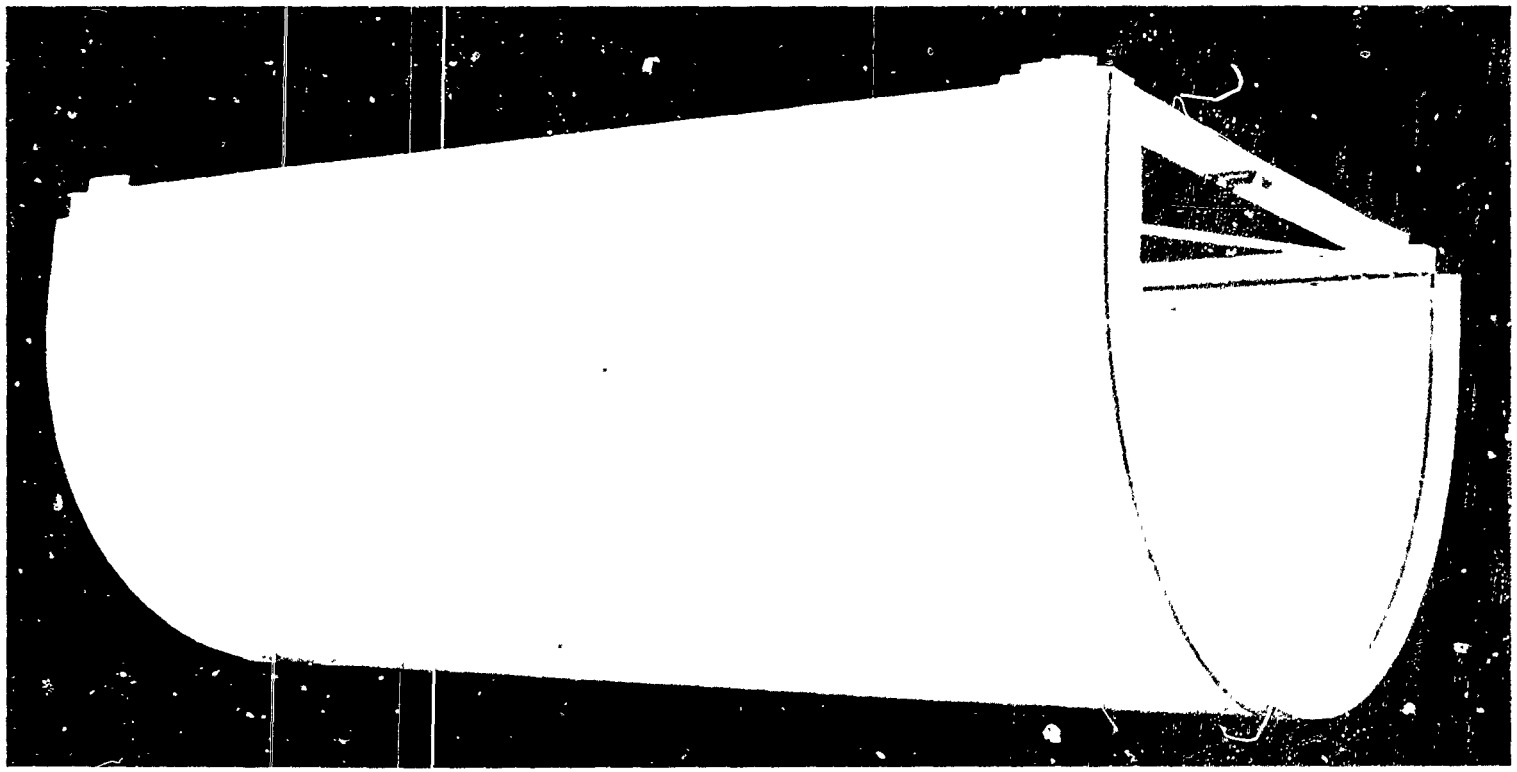

PL\TE 1. CURVED PLATE FOR SKIN FRICTION EXPERIMENT

Contents

Summary

1. Potential flow theory predicts that a body accelerated or decelerated in motion in a straight line in a fluid will experience an inertia force greater than that due to the mass of the body - a so called 'added mass' effect. Submarine trials confirm the phenomenon but indicate that for motion in the fore and aft direction the 'added mass' is much greater than predicted. This could be due to:-

(1) Transient loss of thrust from the propeller,

(2) Changes in skin friction due to the acceleration,

(3) Changes in form drag due to the acceleration.

2. Towing tests have been conducted on a body without propeller. These eliminate (1) as the primary cause.

3. A theoretical and experimental study of (2) has been made for a flat plate. Theory predicts an increase in skin friction for both laminar and turbulent boundary layers, but experiment on the turbulent layer only partially supports the theory. Although further analysis of the data is desirable, the results suggest that acceleration may restore a measure of laminar flow in the boundary layer. Further work should concentrate on this aspect and on the effect of acceleration on form drag.

Approved for issue

Superintendent

THE DRAG OF ANY ACCELERATING SUBMARINE
PART I SKIN FRICTION

By T B Booth

1. INTRODUCTION

An accurate knowledge of the acceleration and deceleration of a submarine has become an important aspect of the calculation of safety trajectories - a subject thrown into prominence by the advent of the high speed submarine. Without this knowledge it is not possible to calculate accurately the depth from which a submarine can reach the surface in the event of flooding, neither is it possible to calculate accurately the depth excursion following a hydroplane jam.

It is well known that a body accelerating in a fluid appears to experience an inertia force greater than (mass of the body) x acceleration. This apparent inertia force can be expressed in the form ('virtual mass') x acceleration, the difference between the acual mass and the virtual mass being commonly referred to as 'added mass'. The terms 'virtual mass' and 'added mass' are unfortunate, being historically associated with the concept of 'entrained water' ie water dragged along with the submarine (in addition to free flooding water trapped within the form which is legitimately part of the dynamical mass of the submarine). The increase in inertia is in fact due to the need to increase the kinetic energy of the fluid whenever the velocity of the body is increased. Lamb (Reference 1) obtained theoretical solutions, based on the work of Green (Reference 2), for the kinetic energy stored in the inviscid potential flow round an ellipsoid. He showed that the excess of the inertia force over (mass of the body) x acceleration, could, for acceleration along a principal axis, be expressed in the form

k x (mass of fluid displaced) x acceleration

where k is a constant whose value depends on the axis concerned, and which he refers to as an 'inertia coefficient'. He obtained similar coefficients for angular accelerations. The 'added mass' and the 'inertia coefficient' are related by:

added mass = k x (mass of fluid displaced)

Note that the inertia coefficient factors the mass of fluid displaced ie the form displacement, which is not necessarily the same as the mass of the body. Reference 3 gives the values of the inertia coefficients, calculated according to Lamb's theory, for a wide range of proportions of ellipsoids.

The limitations of potential flow theory are well known, and until the invention of the Planar Motion Mechanism (References 4 and 5) there was little experimental data concerning the inertia coefficients of a body in water. We now know that Lamb's predictions of the inertia coefficients for vertical and lateral motions are of the correct order when applied to modern submarine shapes, and may be as high as 0.9. There is no doubt that for these motions, inviscid potential flow accounts for nearly all of the increased inertia.

When applied to the forward motion of a submarine, Lamb's theory predicts very small values of k, typically less than 0.05 and this as we shall see is far too low. It is this discrepancy which is the subject of this note.

The first computations of submarine acceleration and deceleration at AEW were carried out some ten years ago, and, in common with practice elsewhere, the inertia coefficient for fore and aft motion was based on that predicted by Lamb, replacing the submarine by an equivalent spheroid, while propeller thrust was based on quasi-steady state values. (There is, in fact, some justification for this practice in Reference 6, in which the inertia coefficient was obtained experimentally from a drop test in water of a body of fineness ratio 3.5. The value of k was deduced to be 0.04, which is less than the theoretical value based on Lamb.)

Some full scale data became available in late 1967 in the form of acceleration and deceleration runs of HMS VALIANT for which the velocity and rpm were recorded against time. Although not entirely satisfactory, and having rpm time histories which differed from those assumed in the predictions, it was evident that the submarine neither accelerated nor decelerated as quickly as predicted.

Opinion at that time attributed the discrepancy to the transient conditions in which the propeller was working compared with the quasi-steady condition assumed in the prediction. Nevertheless the runs were analysed assuming that quasi-steady conditions did apply. Thrust and resistance were estimated using the steady state propeller characteristic and ITTC skin friction values, together with values of 'Taylor Wake', 'Augment' and speed rpm ratios obtained from speed trials, and from them the 'virtual mass' was deduced. This work is reported in Reference 7 from which Figure 1 is taken.

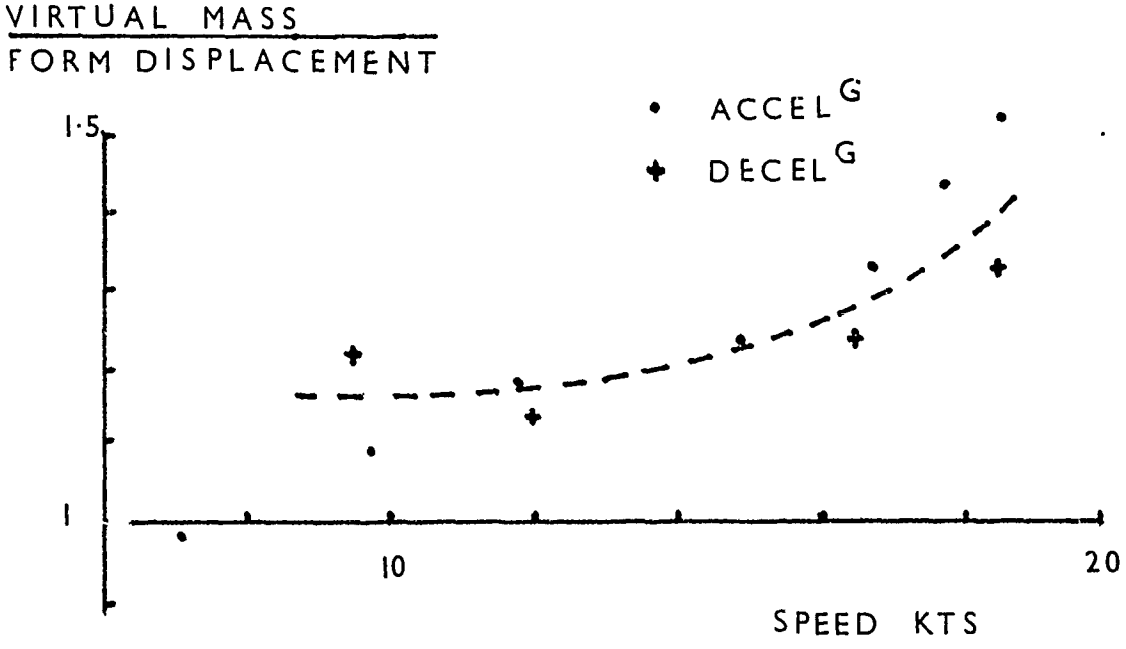

Figure 1. Trials Result

There is some scatter on the results, but, assuming the submarine to have been approximately neutrally buoyant, an inertia coefficient of between 0.15 and 0.4 is indicated. This is too high to be accounted for by the error incurred by treating the submarine as an equivalent ellipsoid.

The high value of inertia coefficient could be due to any of the following:

1. Transient conditions on the propeller and associated effects on the hull causing a loss of thrust.

2. Effects of acceleration and deceleration on the skin friction of the hull.

3. Effects of acceleration and deceleration on the form drag of the hull.

1.1. Propeller Transients

To test the first of these possibilities a submarine model without propeller was towed in No 2 Ship Tank. The resistance, X, was measured during the accelerated and decelerated parts of the tow, as well as at steady speed. Figure 2. Subtracting the steady state drag, D_U, corresponding to the speed at any instant, from the total resistance gives the component due to acceleration. Dividing by the acceleration at that instant gives the 'virtual mass' of the model. Figure 2 shows this to be 10 to 30 per cent of the form displacement. This result, typical of that obtained in several similar experiments on different models, indicates that the propeller is not the primary cause of the phenomenon.

More recently the transient forces on the propeller have been measured (Reference 8) and have been found to be insignificant.*

---

* This conclusion is confirmed by early experiments on airship models, References 9 and 10. The experimenters did not have towing tank facilities and their results are unsatisfactory. Nevertheless they confirm the increase in drag. The reason for the increase appears to have attracted little attention. Presumably interest in airships was waning in favour of fixed wing aircraft.

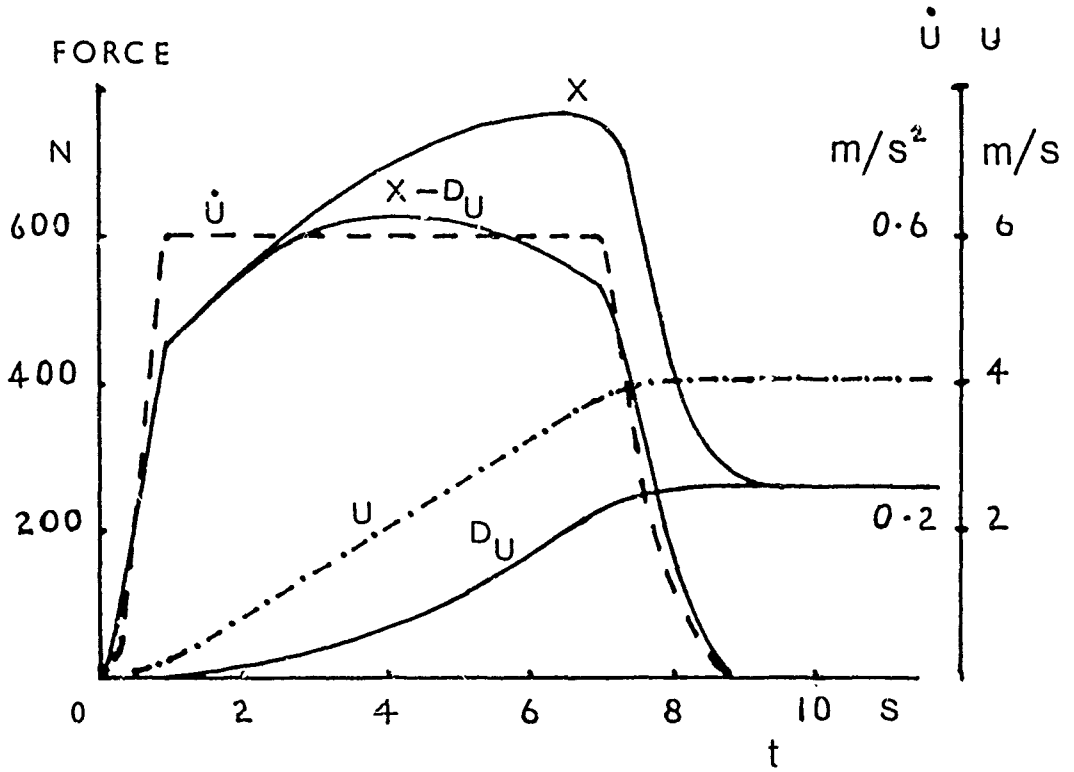

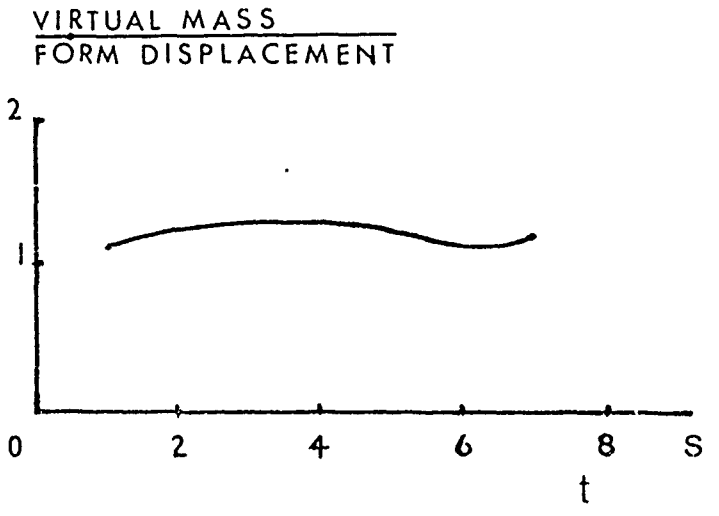

Figure 2. Accelerated Body Experiment

1.2. Form Drag and Skin Friction

The effects of acceleration on both form drag and skin friction merit investigation. The latter has been studied first, partly because there are good reasons to expect that acceleration will increase the skin friction and partly because it is more readily investigated. The results are reported here.

The effects of acceleration on form drag are less clear, and are the subject of future work, which will in due course form a Part II to follow this report.

2. SKIN FRICTION OF AN ACCELERATING PLATE

The derivation of equations of steady state boundary layer flow used in this section is given in Reference 11 or more conveniently in Reference 12.

There is no doubt that the skin friction of a flat plate is increased above the steady state value by acceleration. A simplified physical explanation is as follows.

Suppose a flat plate of infinite span to be in steady motion in its own plane and at right angles to its leading edge so that the velocity profile in the boundary layer at some point P is as shown by curve A on Figure 3.

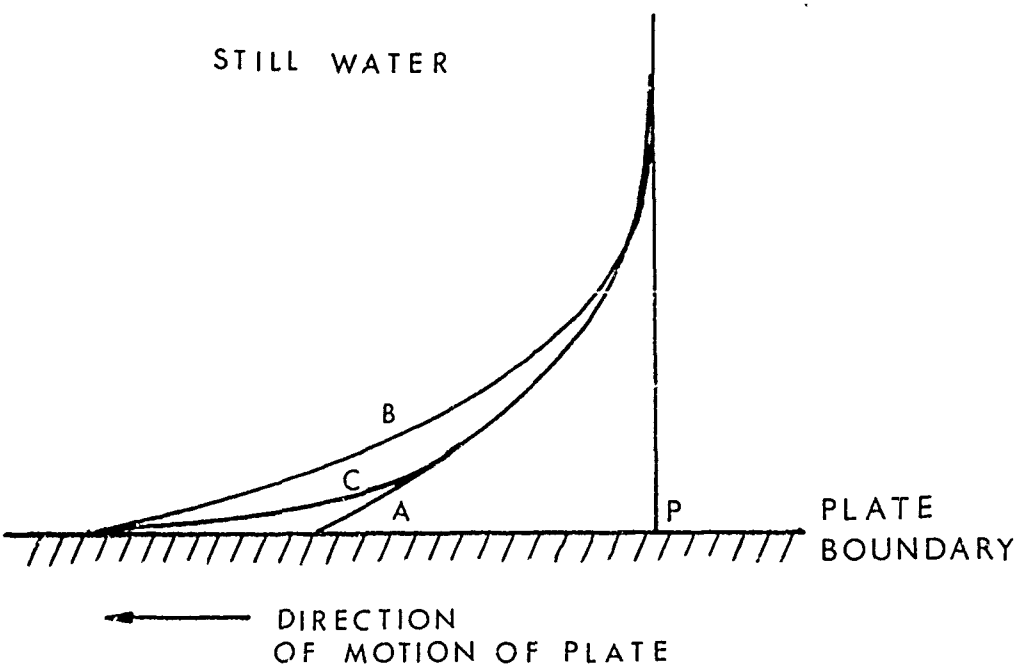

Figure 3. Velocity Profile in the Boundary Layer

Now suppose the plate to be accelerated sharply in the same direction. An instant later the velocity has increased and the velocity profile which would develop at P if this increased velocity were held steady is shown by curve B. But that part of the boundary layer away from the surface of the plate does not have time to develop, so the velocity there remains close to curve A. At the surface of the plate, on the other hand, the velocity in the fluid must increase, on the assumption that the hypothesis of 'no slip' remains true. The actual velocity profile is therefore of the form of curve C. The velocity gradient at the surface is greater than in steady flow and hence the skin friction is greater.

1.1. Notation

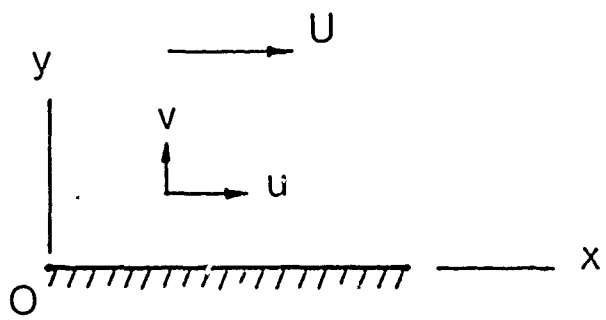

Figure 4

Oxy	Axes fixed in the plate.
	O origin at the leading edge. x co-ordinate along the plate. y co-ordinate normal to the plate.
l b t	Length; breadth; thickness of the plate.
ρ μ ν	Density; viscosity; kinematic viscosity of the fluid.
U $\dot{U}$	Velocity; acceleration of the undisturbed stream relative to the plate.
u v	Velocity components in the boundary layer at (x , y) relative to the plate.
δ	Boundary layer thickness.
δ_1	Displacement thickness $\int_0^\delta (1 - u/U)dy$

θ	Momentum thickness $\int_0^\delta (1 - u/U)\,(u/U)dy$.
R_x R_l	Ux/ν, Ul/ν.
D D_U $D_{\dot{U}}$	Drag; drag at constant speed U; drag due to acceleration = $D - D_U$.
τ τ_U $\tau_{\dot{U}}$	Local skin friction per unit area; etc.
F F_U $F_{\dot{U}}$	Skin friction of one side of a flat plate; etc.
C_f	Mean skin friction coefficient of a flat plate (one side) = $F_U/\frac{1}{2}\rho U^2$ lb.

3. LAMINAR BOUNDARY LAYER

3.1. Equations of Motion

The equations of motion are conveniently established by considering the plate to be stationary in an accelerating stream. In order to accelerate the stream it is necessary to introduce a pressure gradient in the direction of flow of magnitude $-\rho\dot{U}$ where $\dot{U}$ is the acceleration of the undisturbed stream. Hence for two dimensional motion the usual equation of motion

$$\frac{\partial u}{\partial t} + u\frac{\partial u}{\partial x} + v\frac{\partial u}{\partial y} = -\frac{1}{\rho}\frac{\partial p}{\partial x} + \nu\frac{\partial^2 u}{\partial y^2} \qquad (1)$$

becomes

$$\frac{\partial u}{\partial t} + u\frac{\partial u}{\partial x} + v\frac{\partial u}{\partial y} = \dot{U} + \nu\frac{\partial^2 u}{dy^2} \qquad (2)$$

The equations of continuity and laminar skin friction remain unchanged

$$\frac{\partial u}{\partial x} + \frac{\partial v}{\partial y} = 0 \qquad (3)$$

$$\tau = \mu\left(\frac{\partial u}{\partial y}\right)_{y=0} \qquad (4)$$

3.2. Exact Solution

The equations have been solved exactly for a plate of length 4.6 m accelerated from rest in water at 0.6 m/s^2, by the computation described in Appendix I. After the plate has travelled a distance of three lengths the speed is held constant (4.104 m/s). The growth of skin friction at three points, distant 1/5, 21/5 and 41/5 from the leading edge is shown in Figure 5. The points at 1/5 and 41/5 were selected to be free of any error which might arise nearer the leading and trailing edges due to the computing singularities which occur there.

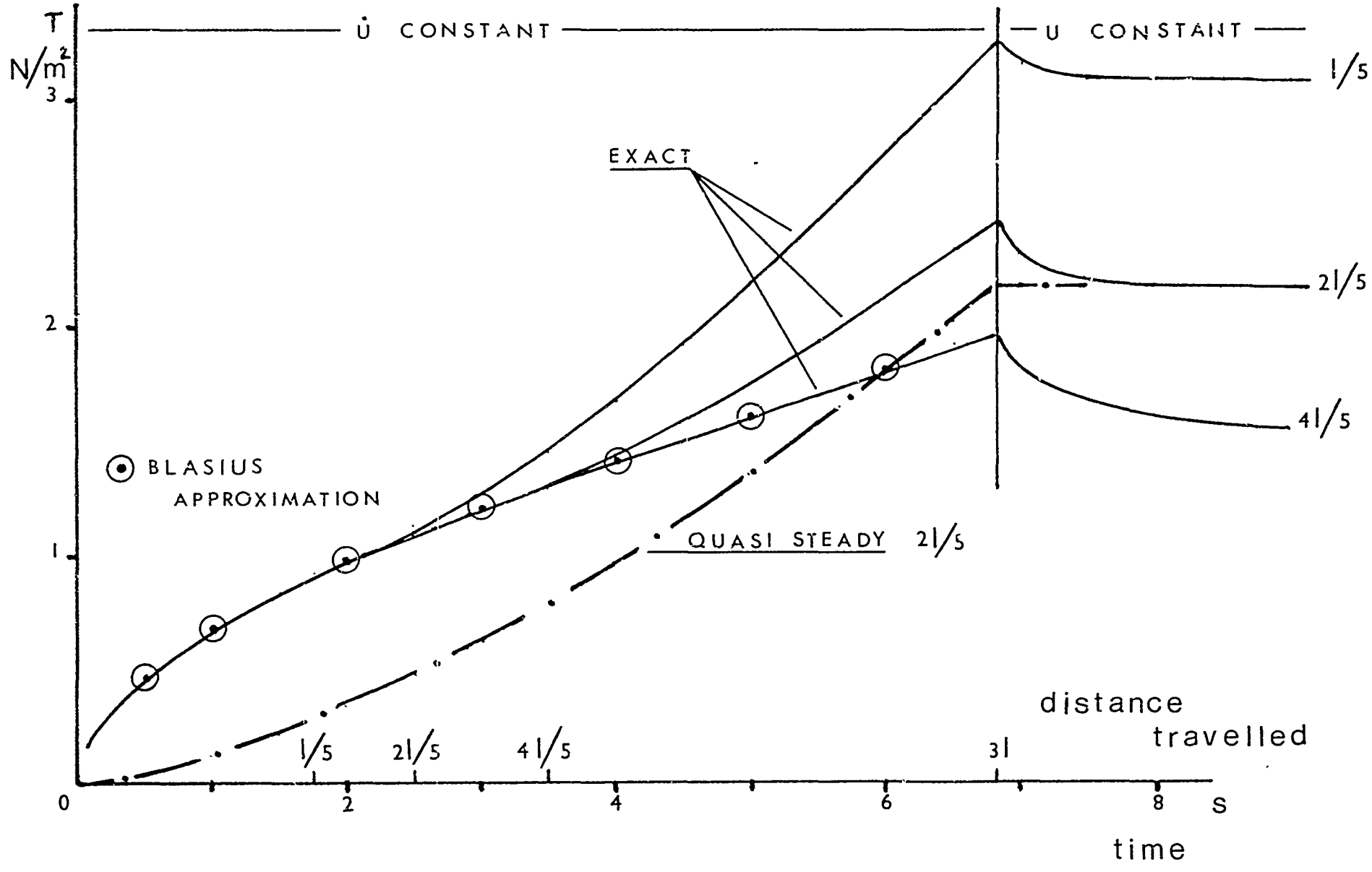

Figure 5. Skin Friction of the Laminar Boundary Layer
$l = 4.6$ m, $\dot{U} = 0.6$ m/s^2

3.3. Quasi Steady Solution

The simplest possible solution is to assume that the skin friction at any instant is that corresponding to fully developed steady flow at the instantaneous speed. This amounts to ignoring the effects of acceleration and cannot be expected to give the correct value, but it is of interest since comparison with the exact solution isolates the effects of acceleration.

The skin friction is given by the well known solution for steady laminar boundary layer flow (References 12 and 11).

$$\tau_U = 0.332\rho U^2(\nu/Ux)^{\frac{1}{2}} \qquad (5)$$

The value at the point 21/5 is given in Figure 5 and shows that, as expected, the quasi steady value is an underestimate. The effect of acceleration dominates in the early stages, reducing as the acceleration continues, the effect being greatest on the rear parts of the plate. It is clear that the increase of skin friction due to acceleration is not constant and that the concept of a constant 'added mass' does not apply to viscous effects.

3.4. Blasius Solution

An approximate solution for constant acceleration from rest was given by Blasius based on the omission of the convection term $u\frac{\partial u}{\partial x}$ from the equation of motion (1).

$$u = U\{-2\eta^2 + 2\pi^{-\frac{1}{2}}\eta e^{-\eta^2} + (2\eta^2 + 1)\mathrm{erf}\,\eta\} \qquad (6)$$

where $\eta = (y/2)/(\nu t)^{\frac{1}{2}}$ $\quad \mathrm{erf}\eta = \int_0^\eta e^{-\alpha^2}\,d\alpha$ (7) (8)

The solution is independent of x, the distance from the leading edge of the plate and leads to uniform skin friction given by

$$\tau = \mu\left(\frac{\partial u}{\partial y}\right)_{y=0} = 2\mu U/\sqrt{\pi\nu t} = 2U(\rho\mu t/\pi)^{\frac{1}{2}} \qquad (9)$$

The Blasius solution agrees very well with the exact solution in the early stages of the motion (Figure 5). As the acceleration continues agreement remains good at the point x = 41/5, but underestimates skin friction at the forward points, being about 40 per cent low at the point x = 1/5 at the end of the accelerated motion. Clearly the convection terms omitted in the Blasius approximation can have an important effect on the forward part of the plate.

A physical explanation of the discrepancy is as follows. The Blasius solution allows for the development of the boundary layer by diffusion only, leading to uniform conditions over the plate. But the boundary layer also develops by convection from the leading

edge where the boundary layer is thin and the skin friction high. The kinetic energy required for convective development is provided by the work done by increased skin friction. However in the initial stages of the accelerated motion the effects convected from the leading edge do not reach points downstream until those points have travelled approximately to the initial position of the leading edge. Only up to this time can the Blasius solution be expected to apply. The times to travel 1/5, 21/5 and 41/5 are marked on Figure 5 and support this explanation.

3.5. Momentum Theory

An alternative solution may be obtained from the momentum equation

$$\tau/\rho U^2 = \frac{\partial \theta}{\partial x} + (1/U)\frac{\partial U}{\partial x}(2\theta + \delta_1) + (1/U^2)\frac{\partial}{\partial t}(U\delta_1) \qquad (10)$$

where $$\delta_1 = \int_o^\delta (1 - u/U)dy \qquad (11)$$

$$\theta = \int_o^\delta (1 - u/U)(u/U)dy \qquad (12)$$

and in which the terms in $\frac{\partial U}{\partial x}$ vanish in this application.

In steady state flow the following relations are obtained

$$\delta_1 = 1.72\, x(R_x)^{-\frac{1}{2}} \qquad (13)$$

$$\frac{\partial \theta}{\partial x} = 0.332\, R_x^{-\frac{1}{2}} \qquad \text{where } R_x = Ux/\nu \qquad (14)$$

and we may assume that these relations still hold when the plate is accelerated. On this assumption, for the accelerating plate

$$\tau/\rho U^2 = 0.332\, R_x^{-\frac{1}{2}} + (1/U^2)\frac{\partial}{\partial t}\{1.72\, x\,(\nu/Ux)^{\frac{1}{2}}U\}$$

$$= 0.332\, R_x^{-\frac{1}{2}}\{1 + 2.59\,(\dot{U}x/U^2)\} \qquad (15)$$

Note that it has not been necessary to assume that the acceleration is constant.

The first term is that due to quasi steady flow while the second is due purely to the acceleration. The contribution of the latter to τ is

$$\tau_{\dot{U}} = 0.332\, R_x^{-\frac{1}{2}}\{2.59\,(\dot{U}x/U^2)\}\rho U^2 = 0.86\rho x\, R_x^{-\frac{1}{2}}\dot{U} \qquad (16)$$

Comparison with the exact solution in Figure 6

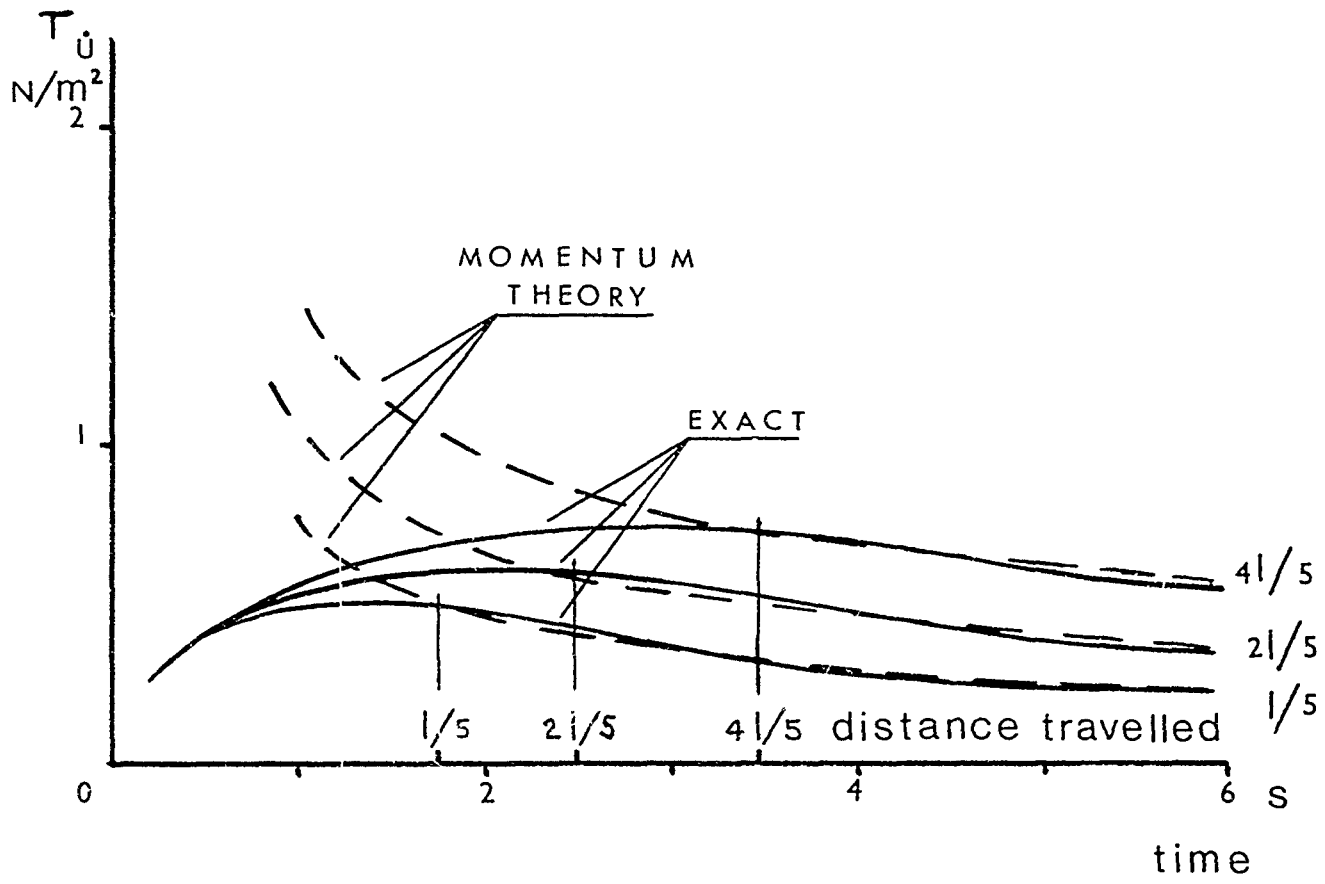

Figure 6. Laminar Boundary Layer Skin Friction Increment
ℓ = 4.6 m, $\dot{V}$ = .6 m/s²

shows remarkably good agreement in the later stages of the motion. It appears that agreement becomes good at a particular point along the plate when that point passes the initial position of the leading edge. Before this occurs the momentum theory overestimates the skin friction.

This is consistent with the discussion of the Blasius solution. The values of δ_1 and τ used in conjunction with the momentum equation are essentially based on a fully convected flow, leading us to expect the agreement which is in fact obtained.

4. TURBULENT BOUNDARY LAYER

Despite the considerable volume of literature on turbulent flow the author is not aware of any simple 'law of turbulence' which can be used to calculate the effect of acceleration on skin friction. However the results of applying the momentum equation to the laminar boundary layer suggest that a similar theoretical approach might be made to the turbulent boundary layer. As a test of the results it is possible, although not easy, to measure the skin friction experimentally on a plate towed at accelerating speed in the towing tank.

4.1. Momentum Theory

Equation (10) is valid for both laminar and turbulent boundary layers

$$\tau/\rho U^2 = \frac{\partial \theta}{\partial x} + (1/U)\frac{\partial U}{\partial x}(2\theta + \delta_1) + (1/U^2)\frac{\partial}{\partial t}(U\delta_1) \qquad (18)$$

in which as before $\frac{\partial U}{\partial x} = 0$.

For Reynolds Numbers of the order of 10^6 the 'seventh power law'

$$u/U = (y/\delta)^{1/7} \qquad (19)$$

is known to give a good approximation to the velocity in the turbulent boundary layer leading to expressions for δ_1 and θ (Reference 12)

$$\delta_1 = 0.0463\, xR_x^{-1/5} \qquad (20)$$

$$\theta = 0.036\, xR_x^{-1/5} \qquad (21)$$

On substituting in (18)

$$\tau/\rho U^2 = 0.0288\, R_x^{-1/5}\{1 + 1.285\,(\dot{U}x/U^2)\} \qquad (22)$$

and on integrating the skin friction F of a width b of <u>one</u> side of a plate of length l is given by

$$C_f = F/(\tfrac{1}{2}\rho U^2 lb) = (2/l)\int_0^l (\tau/\rho U^2)dx$$

$$= 0.072\, R_l^{-\frac{1}{2}}\{1 + 0.572\,(\dot{U}l/U^2)\} \qquad (23)$$

The first term is the steady state skin friction, while the second term is due to acceleration. The latter can be written in the form

$$F_{\dot{U}}/\tfrac{1}{2}\rho\dot{U}l^2b = 0.058\,4\ R_l^{-1/5} \qquad (24)$$

Since R_l contains U this form does not lead us to expect that the 'added mass' will be constant.

5. TOWED PLATE EXPERIMENT

It would appear a simple matter to measure the resistance of a plate towed in its plane in a fluid at accelerating speed, and for this purpose the No 2 Ship Tank carriage at AEW is well suited, having a reasonably constant acceleration until approaching the ordered speed. In practice considerable care is needed if the measurements are to be free of contamination from the effects of roughness, waviness, edge and free surface effects, support interference, thickness effect, distortion and misalignment of the plate (see for example Hughes Reference 13). In particular, if a thin plate is towed in a vertical position by a support which is clear of the fluid, that part of the leading edge away from the support is liable to deflect and possibly break. Dr Hughes devised a special rig which enabled him to monitor such deflections, and this is satisfactory for a steady tow, but greatly increases the towed mass. In the present experiment this is not acceptable since, during the accelerated motion, the hydrodynamic resistance will have to be extracted from a gauge measurement which already includes large inertia forces.

This difficulty has been overcome by towing a plate curved into a a U section (see Figure 7 and Plate 1) the radius of which is large compared with the boundary layer thickness.

As can be seen from section 5.1 the 'Experiment Details' this configuration makes possible tests up to a Reynolds Number of 6.5×10^6 on a plate of considerable area and rigidity, yet having a thickness/length ratio of less than 0.5 per cent and an effective aspect ratio (2 x immersed perimeter/length, as defined by Dr Hughes) of 1.97. The radius of the U was chosen to permit the plate to enter the dock of No 2 Ship Tank, but there seems to be no reason to prevent plates of larger radius being tested at higher speeds.

The plate is a sandwich. Two 4 mm sheets of plywood, curved over a forming mould and glued together, are sandwiched between sheets of 'Formica'. This form of construction ensures a smooth finish free from waviness, and eliminates changes of mass due to water absorbtion. With the bracing members fitted the plate is extremely rigid. By limiting the length to 2.438 m (8 feet) transverse joins in the Formica are avoided.

With the U configuration care is necessary to ensure vertical alignment as well as fore and aft alignment. The latter was checked during runs by observing the water surface level on the inside and

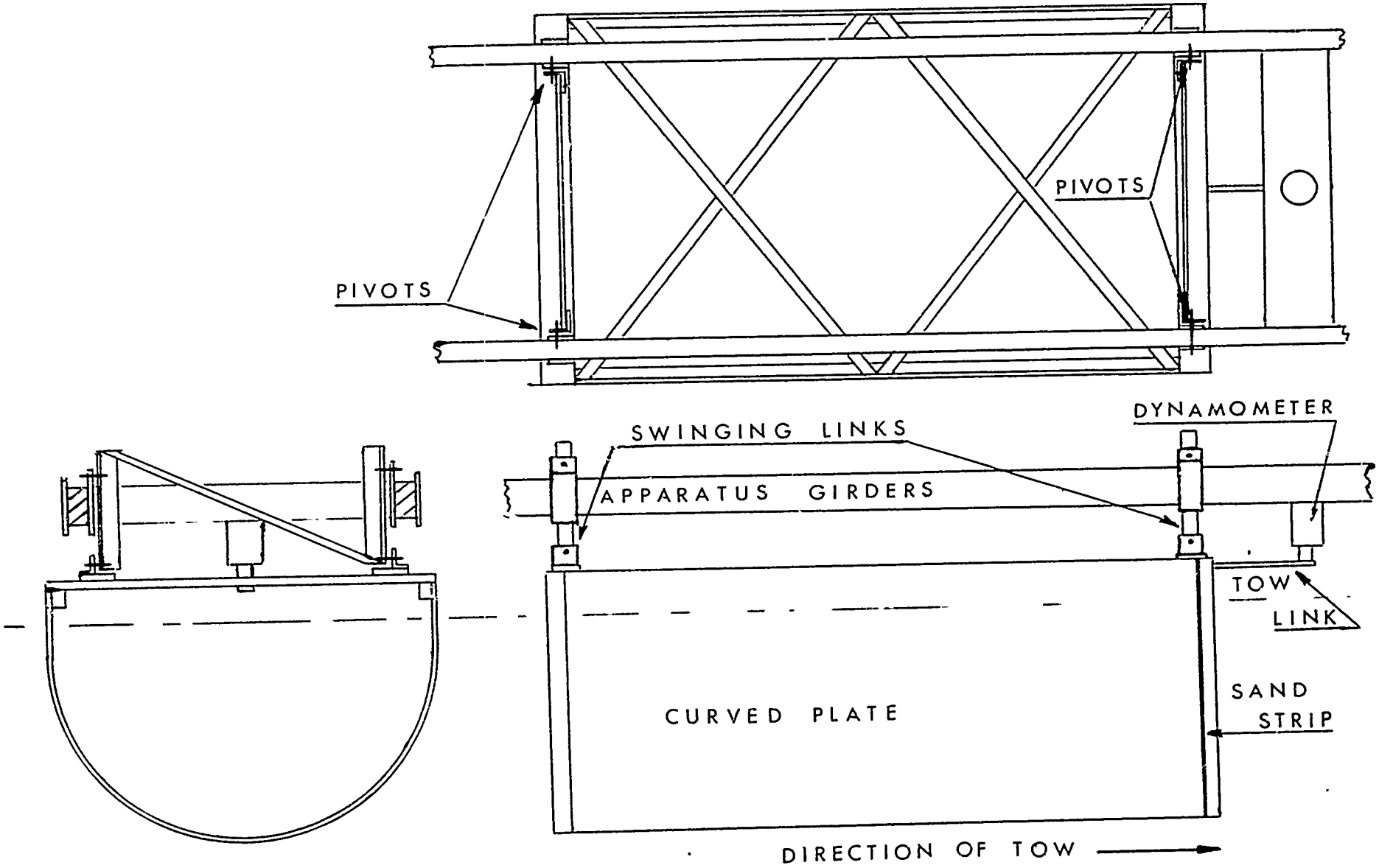

Figure 7. Rig for Towing Curved Plate

outside of the plate. It is also necessary to align the swinging links of the suspension to be accurately vertical, and the towing link to be accurately horizontal. A dynamometer of high stiffness was chosen so as to ensure that the swinging links remained vertical during the tow. The movement of these links was observed and confirmed to be negligible.

5.1. Experiment Details

Curved Plate

Length	2.438 m
Radius (outer skin)	711 mm
Immersed perimeter (outer)	2.405 m
Wetted area (both sides)	11.635 m^2
Thickness	11.5 mm
Thickness/length ratio	0.47 per cent
Aspect ratio = $\frac{2 \times \text{wetted perimeter}}{\text{length}}$	1.97
Towed mass	83.83 kg
Surface finish	'Formica'
Turbulence stimulation	Sand strip 1/8 inch x 0.0014 inch grains

Instrumentation

Carriage speed - a. From feedback tachometer on carriage wheels recorded on U/V recorder.

b. At steady speed, by time between fixed points, electronic measurement displayed digitally.

Carriage acceleration - from accelerometer, recorder on U/V recorder.

Towing force - by strain gauged post dynamometer, recorded on U/V recorder.

Schedule of Runs

Runs were made at various accelerations, up to 0.05 g maximum. Each run consisted of an acceleration from rest, the acceleration being reasonably constant, up to various speeds (maximum 3.048 m/s) at which the speed was held constant for several lengths. Maximum Reynolds Number attained 6.5×10^6.

5.2. Steady State Skin Friction

The steady state skin friction coefficient is plotted in Figure 8. These values have been corrected as in Reference 13 for form drag and turbulence stimulation as follows.

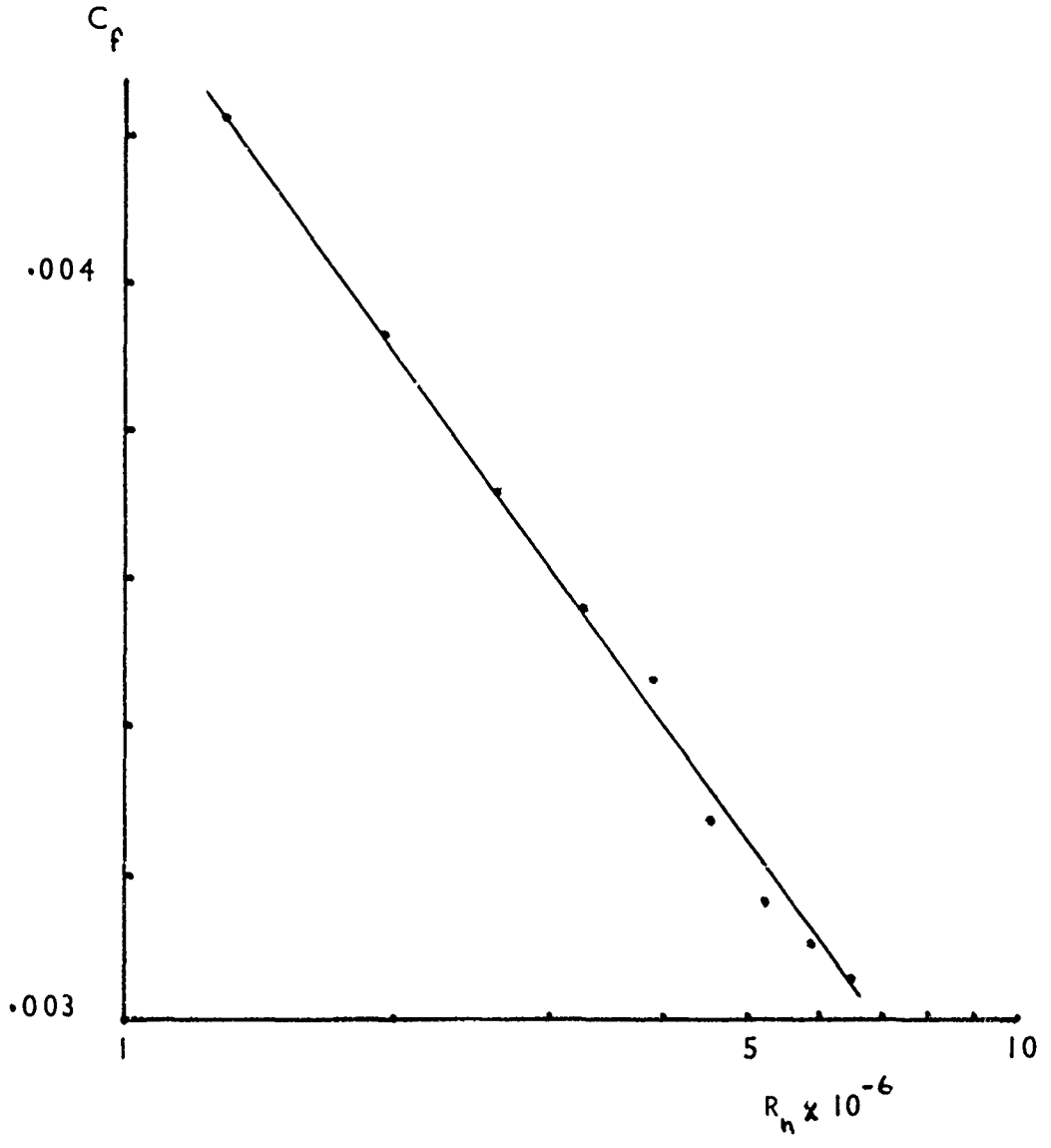

Figure 8. Curved Plate - Steady State Skin Friction Coefficient

Form drag correction (per cent) = 3 x thickness/length ratio (per cent)

Turbulence stimulation correction = 0.04

Air drag was measured by towing a duplicate rig less the in-water part.

The results are consistent with those presented in Reference 13.

5.3. Effect of Acceleration

The steady state drag (uncorrected) corresponding to the instantaneous speed has been subtracted from the measured resistance, as has also the inertia resistance of the plate and mountings leaving the hydrodynamic drag due to acceleration. Points from a number of runs are plotted in non-dimensional form in Figure 9.

There is a good deal of scatter on the results, but it is nevertheless clear that the momentum theory overestimates the effect. At the higher speeds the effect appears to be negative, suggesting that turbulent flow may be suppressed during the accelerated motion. However this conclusion must be treated with reserve since a discrepancy has been detected in the measurement of the acceleration. It is intended to reanalyse some of the points, but this is unlikely to upset the general conclusion that the momentum theory overestimates the skin friction. We may further conclude that such increase in skin friction as occurs is not sufficient to account for the increase in drag of the submarine. Thus attention should also be directed to the effect of acceleration on form drag.

6. CONCLUSIONS

6.1. The increase of skin friction of the laminar boundary layer a plate due to acceleration is well represented by

a. Blasius solution during the early stages of the motion ie before the plate has travelled one length.

b. Momentum theory during the later stages ie after the plate has travelled one length.

6.2. Applying momentum theory based on the seventh power law to the turbulent boundary layer of an accelerating plate gives skin friction values greater than those measured experimentally. It is possible that acceleration suppresses turbulent flow in the boundary layer, but some reanalysis of data is needed to resolve a discrepancy in the measurement of acceleration.

6.3. Skin friction increases do not appear to be large enough to account for the increased drag of a submarine during acceleration. Attention should now be directed to the effects on form drag.

ACKNOWLEDGEMENT

Mr J Anslow's contribution to discussions leading to the curved plate experiment is acknowledged.

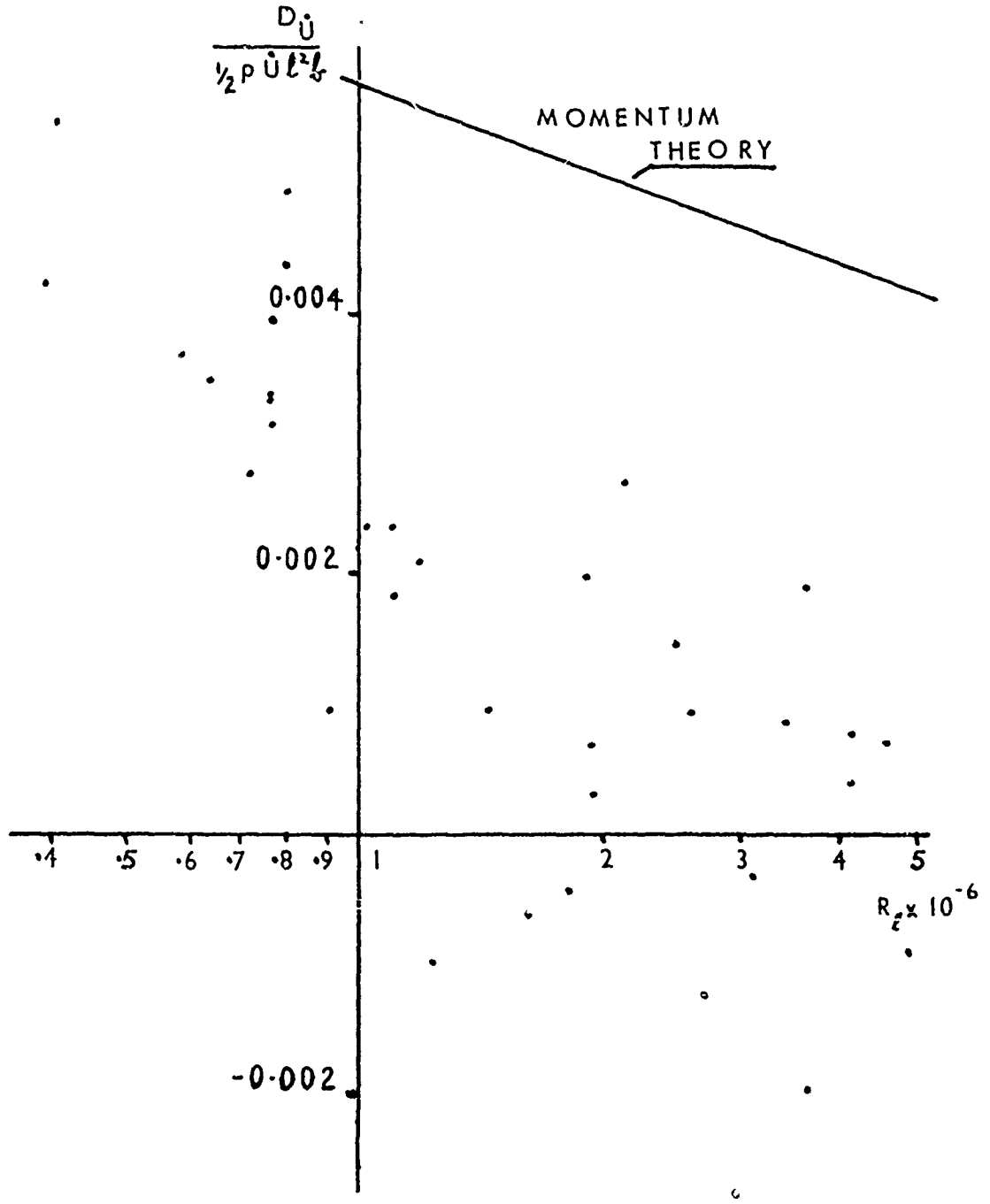

Figure 9. Curved Plate - Drag Increment Due to Acceleration

References

Reference 1. Lamb H. The Inertia Coefficients of an Ellipsoid Moving in a Fluid. ARC 1918-9 R and M 623. (Also Lamb - Hydrodynamics p.) UNCLASSIFIED.

Reference 2. Green G. Research on the Vibration of Pendulums in Fluid Media. Trans R S Edin xiii, 54 (1883) (papers p 315). UNCLASSIFIED.

Reference 3. Kochin N E, Kibel I A, Roze N V. Theoretical Hydrodynamics. Interscience Publishers (Wiley) 1964. UNCLASSIFIED.

Reference 4. Gertler M. Paper 6. Symposium on Towing Tank Facilities Instrument and Measurement Technique, Zagreb 1959. UNCLASSIFIED.

Reference 5. Booth T B, Bishop R E D. The Planar Motion Mechanism. Published AEW 1973. UNCLASSIFIED.

Reference 6. Cowley W L, Levy H. On the Effect of Acceleration of Bodies on their Air Resistance. ARC R and M 612, 1918-9. UNCLASSIFIED

Reference 7. Unpublished AEW Report.

Reference 8. Investigation into the Behaviour of Marine Propellers when Subjected to Dynamic Loading Conditions. MIC Report CS 236. December 1974. UNCLASSIFIED

Reference 9. Frazer R A, Simmons L F G. Dependance of the Resistance of Bodies upon Acceleration as Determined by Chronograph Analysis. ARC R and M 590. UNCLASSIFIED.

Reference 10. Relf E F, Jones R. Measurement of the Effect of Accelerations on the Longitudinal and Lateral Motions of an Airship. ARC R and M 613. UNCLASSIFIED.

Reference 11. Blasius H, Zeitschr. Fur Mathematik and Physik. 56 (1908), 20-37. UNCLASSIFIED.

Reference 12. Goldstein S. Modern Developments in Fluid Dynamics. OUP. UNCLASSIFIED.

Reference 13. Hughes G. Frictional Resistance of Smooth Plane Surfaces in Turbulent Flow - New Data and a Survey of Existing Data - Trans INA 1952 Vol 94 p 287. UNCLASSIFIED

Appendix I

LAMINAR BOUNDARY LAYER COMPUTATION

Equations (2), (3) and (4) are computed, viz

$$\frac{\partial u}{\partial t} + u\frac{\partial u}{\partial x} + v\frac{\partial u}{\partial y} = \dot{U} + \nu\frac{\partial^2 u}{\partial y^2}$$

$$\frac{\partial u}{\partial x} + \frac{\partial v}{\partial y} = 0$$

$$\tau = \mu\left(\frac{\partial u}{\partial y}\right)_{y=0}$$

for the conditions:

At the surface of the plate $u = v = 0$

Well away from the plate $u = U$, the free stream velocity relative to the plate.

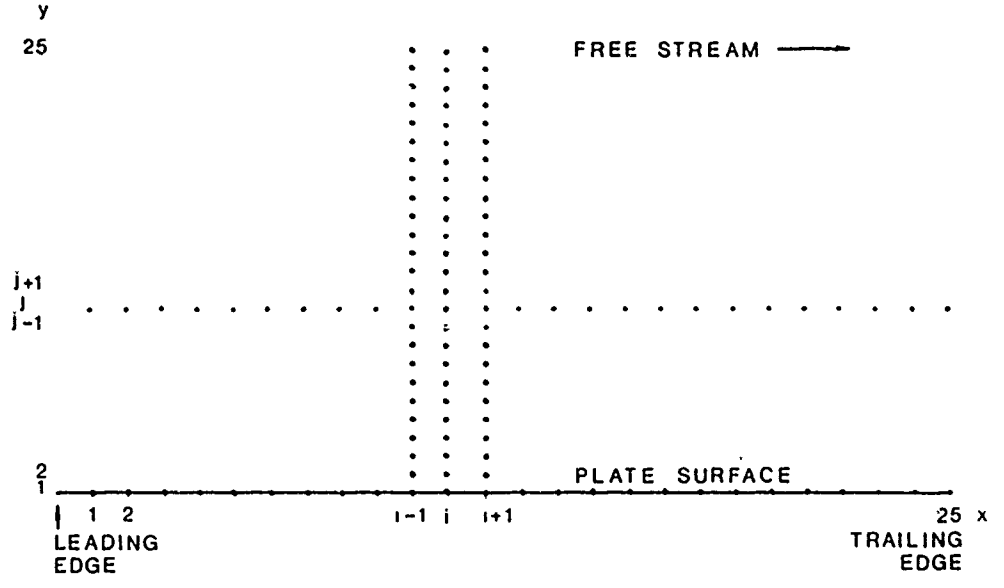

The value of u is stored for each of 25 values of y at each of 25 stations of x. The x sections divide the length of the plate into 25 equal intervals, DX = 1/25, so that the x co-ordinate of the ith station is x_i = i DX where i = 1,25. (A station is not required at the leading edge, since this is a singular point at which no computing is possible or required.) The y values are equally spaced, DY, so that y_j = (j - 1)DY where j = 1,25. Thus j = 1 is

the surface of the plate. The value of DY may be chosen as thought appropriate - in this instance DY = 0.001 DX.

The solution is iterated at time interval DT which may be chosen or programmed as appropriate - in this instance DT = 0.01 seconds. (Note that too long an iteration interval causes instability in the computation.)

In addition to the main file which stores all 625 values of u, four working arrays U1, U2, U3, U4 of dimension 25 each are used. The equations of motion are evaluated at each x station in turn. When the ith station is being evaluated the existing velocity profiles at x_{i-1}, x_i, x_{i+1} are stored in U1, U2, U3 respectively. The updated velocity profile at i is stored in U4 whence it is written into the main file. Having completed the evaluation of the ith station the contents of U2 are transferred to U1, those of U3 to U2, and the velocity profile at i + 2 is read from the main file to U3 in readiness for the evaluation of station i + 1.

For each value of y at a given x station the value of $\frac{\partial u}{\partial t}$ is computed from the equation of motion (2), having first computed $\frac{\partial u}{\partial x}$, $\frac{\partial u}{\partial y}$, $\frac{\partial^2 u}{\partial y^2}$ and v.

The partial differentials are computed by simple differences for values of j from 2 to 24. (Values at j = 1 and 25 are not needed for the computation of u since u = 0 at j = 1, and has the free stream value at j = 25.)

$$\frac{\partial u}{\partial x} = \tfrac{1}{2}\,(U3_j - U1_j)/DX = UX_j \text{ say}$$

$$\frac{\partial u}{\partial y} = \tfrac{1}{2}\,(U2_{j+1} - U2_{j-1})/DY$$

$$\frac{\partial^2 u}{\partial y^2} = (U2_{j+1} - 2\,U2_j + U2_{j-1})/(DY)^2$$

The singularity at the leading edge makes it impossible to compute the velocity profile at the first x station. It is assumed that the boundary layer at this station develops very quickly so that the velocity profile is that corresponding to steady state at the instantaneous speed. A similar difficulty arises at station 25 (the trailing edge) since it is not possible to compute $\frac{\partial u}{\partial x}$ at this station.

Strict precision required the computation to be continued downstream of the trailing edge, however $\frac{\partial u}{\partial x}$ is small near the trailing edge and it is sufficiently accurate to base $\frac{\partial u}{\partial x}$ there on the difference in u between stations 24 and 25.

v is computed from the equation of continuity (3) by integration of $\frac{\partial u}{\partial x}$ using a trapezium rule and the condition that at the surface of the plate $v = \frac{\partial u}{\partial x} = 0$

$$v_j = \sum_{j=2}^{j} \tfrac{1}{2}(UX_{j-1} + UX_j)D_1$$

Since u is zero at the surface of the plate the skin friction at station i is given from (4) by

$$\tau_i = \mu(u_{j=2})_i/DY$$

Values of τ_i are stored in an array UYO of dimension 25, the contents of which are printed when all 25 x station have been updated.

After printing output as required, the time, distance travelled by the plate velocity are updated in preparation for the next iteration. It is not necessary that the plate acceleration should be constant - in this instance the plate acceleration is set to zero when the plate has travelled through three lengths.

Distribution

Copy Numbers	1-5	Director General Ships (For attention of DWD)
	6	Superintendent AEW
	7	Staff Officer (C) BNS
	8-14	US Navy Technical Liaison Officer
	15-19	CDRS(L)
	20	Director ARL
	21-36	DRIC

DOCUMENT CONTROL SHEET

(Notes on completion overleaf)

Overall security classification of sheet ..... UNCLASSIFIED .....

(As far as possible this sheet should contain only unclassified information. If it is necessary to enter classified information, the box concerned must be marked to indicate the classification eg (R),(C) or (S))

1. DRIC Reference (if known)	2. Originator's Reference	3. Agency Reference	4. Report Security Classification
	AEW-TR-76003		UNCLASSIFIED

5. Originator's Code (if known)	6. Originator (Corporate Author) Name and Location
	SUPERINTENDENT ADMIRALTY EXPERIMENT WORKS HASLAR GOSPORT HANTS PO12 2AG
5a. Sponsoring Agency's Code (if known)	6a. Sponsoring Agency (Contract Authority) Name and Location

7. Title THE DRAG OF AN ACCELERATING SUBMARINE PART I SKIN FRICTION

7a. Title in Foreign Language (in the case of translations)

7b. Presented at (for conference papers). Title, place and date of conference

8. Author 1, Surname, initials	9a Author 2	9b Authors 3, 4...	10. Date	pp	ref
BOOTH T B			1.1976	28	13

11. Contract Number	12. Period	13. Project	14. Other References

15. Distribution statement

CONDITION OF RELEASE - UNLIMITED

Descriptors (or keywords)

ACCELERATION
DRAG
RESISTANCE
SKIN FRICTION
SUBMARINES

Abstract

Both full scale trial and towing tank experiment show that the 'virtual mass' in the fore and aft direction is greater than that predicted by potential flow theory. This report examines the increase in skin friction due to acceleration. A later report will examine the effect of acceleration on form drag.